Signature of multiradical character in second hyperpolarizabilities of rectangular graphene nanoflakes

ARTICLE *in* CHEMICAL PHYSICS LETTERS · APRIL 2010

Impact Factor: 1.9 · DOI: 10.1016/j.cplett.2010.03.013

11 AUTHORS, INCLUDING:

Masayoshi Nakano
Osaka University
337 PUBLICATIONS **4,785** CITATIONS
SEE PROFILE

Ryohei Kishi
Osaka University
110 PUBLICATIONS **1,948** CITATIONS
SEE PROFILE

Edith Botek
Belgian Institute for Space Aeronomy
104 PUBLICATIONS **2,283** CITATIONS
SEE PROFILE

Benoît Champagne
University of Namur
401 PUBLICATIONS **8,737** CITATIONS
SEE PROFILE

Chemical Physics Letters 489 (2010) 212–218

Contents lists available at ScienceDirect

Chemical Physics Letters

journal homepage: www.elsevier.com/locate/cplett

Signature of multiradical character in second hyperpolarizabilities of rectangular graphene nanoflakes

Hiroshi Nagai [a], Masayoshi Nakano [a,*], Kyohei Yoneda [a], Ryohei Kishi [a], Hideaki Takahashi [a], Akihiro Shimizu [b], Takashi Kubo [b], Kenji Kamada [c], Koji Ohta [c], Edith Botek [d], Benoît Champagne [d]

[a] Department of Materials Engineering Science, Graduate School of Engineering Science, Osaka University, Toyonaka, Osaka 560-8531, Japan
[b] Department of Chemistry, Graduate School of Science, Osaka University, Toyonaka, Osaka 560-0043, Japan
[c] Photonics Research Institute, National Institute of Advanced Industrial Science and Technology (AIST), Ikeda, Osaka 563-8577, Japan
[d] Laboratoire de Chimie Théorique, Facultés Universitaires Notre-Dame de la Paix (FUNDP), rue de Bruxelles, 61, 5000 Namur, Belgium

ARTICLE INFO

Article history:
Received 13 February 2010
In final form 2 March 2010
Available online 6 March 2010

ABSTRACT

Using spin-unrestricted density functional theory methods, the second hyperpolarizabilities, γ, of rectangular graphene nanoflakes of different sizes have been investigated for their singlet ground state in conjunction with their open-shell character. It is shown that their multiradical nature leads to a unique dependence of the γ component along the armchair edges and that this behavior can be rationalized not only in terms of the diradical character (y_0) derived from the HOMO and LUMO occupation numbers, but also in terms of the one (y_1) derived from the HOMO−1 and LUMO+1 ones: the γ components are enhanced when the systems take intermediate y_1 values in addition to intermediate y_0 values.

1. Introduction

Nanographenes – single atomic layers of nanographite – have attracted a great interest because of their unique electronic and spin properties, and are therefore expected to form a new class of materials in order to achieve future nanoscale devices in the fields of electronics, photonics and spintronics [1–11]. For example, recent theoretical and experimental studies have elucidated their fascinating properties such as massless quasi-particles [3], room-temperature quantum hall effect [4], half-metallicity [5] and unique magnetic properties [7–16]. Theoretical studies on nanographenes with low-dimensional structures, e.g., one-dimensional ribbons [7–16], two-dimensional few-layer graphites [17], and finite-size nanoflakes with triangular, rectangular and hexagonal shapes [18–26], predict that the electronic, vibrational, transport, and spin properties of graphenes significantly change as going to lower dimensions. These changes often originate in the edge effects, e.g., zigzag-edged one-dimensional graphene nanoribbons possess open-shell singlet ground states in contrast to armchair-edged ones having closed-shell ground states.

In the course of recent investigations on the nonlinear optical (NLO) properties, it turned out that substantial enhancements can be achieved in open-shell compounds [27–31] and that spin multiplicity can control the amplitude of the second hyperpolarizability (γ) – the microscopic origin of the third-order NLO properties. In particular, singlet diradical compounds [32] display a unique structure–property relationship between γ and the diradical character (y): for singlet diradical systems, γ increases with y until it attains a maximum in the intermediate diradical character region, then it decreases [33–36]. This dependence of γ has been exemplified by ab initio molecular orbital (MO) and density functional theory calculations on various model and real systems including diphenalenyl radicals [33,35,37,38] and graphene nanoflakes [39,40] as well as by two-photon absorption (TPA) measurements on polyaromatic diphenalenyl diradicaloids [41]. Preliminary investigations on nanographenes have also shown that they can display outstanding NLO responses in relation with their multiradical character. Hachmann, Jiang, and co-workers have also theoretically predicted that higher acenes present a singlet multiradical ground state [14,26] while we recently showed that a square graphene nanoflake, i.e., polycyclic aromatic hydrocarbon, PAH[5,5], possesses not only nearly a pure diradical character but also somewhat tetraradical character [39]. Considering these features, we expect that large size rectangular graphene nanoflakes display singlet multiradical ground states and that their multiradical character will impact the γ values. Therefore, in order to assess the relationship between the multiradical character and γ, we investigate in this Letter the two dominant diagonal components of γ (along the zigzag and armchair edges) for rectangular graphene nanoflakes (PAHs) of different sizes.

* Corresponding author. Fax: +81 6 6850 6268.
E-mail address: mnaka@cheng.es.osaka-u.ac.jp (M. Nakano).

0009-2614/$ - see front matter © 2010 Elsevier B.V. All rights reserved.
doi:10.1016/j.cplett.2010.03.013

2. Methodology

2.1. Model systems and diradical characters

Fig. 1 shows the structures of PAH[X,Y], where X and Y denote the number of fused rings in the zigzag and armchair edges, respectively [$1 \leqslant X \leqslant 7$, $1 \leqslant Y$ (odd number) $\leqslant 7$]. The geometries of all systems in their singlet state were optimized using the spin-unrestricted (U) B3LYP/6-31G* method. All singlet optimized geometries belong to the D_{2h} symmetry. The geometries of PAH[1,Y], PAH[2,Y], PAH[3,1], PAH[3,3], PAH[4,1] and PAH[5,1] coincide with those calculated by the spin-restricted (R) B3LYP/6-31G* method, respectively, in contrast to the other cases. This is consistent with the fact that PAHs with short zigzag edges present relatively small diradical characters [obtained from the spin-unrestricted Hartree–Fock (UHF) results] and therefore tend to adopt a closed-shell ground state at the B3LYP level of approximation [39]. The optimized geometries of the zigzag edges exhibit essentially the same features as those of oligoacenes [11,14]. As shown in our previous study [39], in the middle region of the zigzag edges, the rung C–C bonds (in the y-direction) are longer than the ladder C–C bonds (in the x-direction), and the bond-length alternation of the ladder C–C bonds increases toward the ends of the zigzag edges.

We employed the diradical character y_i [related to the HOMO$-i$ and LUMO+i] defined by twice the weight of the doubly-excited configuration in the multi-configurational self-consistent-field theory. In the case of the spin-projected UHF (PUHF) theory it is formally expressed as [42,43]

$$y_i = 1 - \frac{2T_i}{1 + T_i^2}, \tag{1}$$

where T_i is the orbital overlap between the corresponding orbital pair. It can also be expressed in terms of the occupation numbers $[n_j(j = \mathrm{HOMO} - i, \mathrm{LUMO} + i)]$ of UHF natural orbitals (UNOs):

$$T_i = \frac{n_{\mathrm{HOMO}-i} - n_{\mathrm{LUMO}+i}}{2}. \tag{2}$$

y_i represents the diradical character (associated with the HOMO$-i$ and LUMO+i) or the instability of the chemical bond and ranges between 0 (closed-shell) and 1 (pure diradical). The present scheme using the UNOs is the simplest but it can well reproduce the diradical characters calculated by other methods such as the ab initio configuration interaction method [43,44]. It is here noted that the distribution of non-zero values of y_i in the region with $i > 0$ indicates the system having multiradical (beyond diradical) character, e.g., $y_0 = y_1 = 1$ [and $y_i = 0$ ($i > 1$)] means that the system has a pure tetraradical character as a whole.

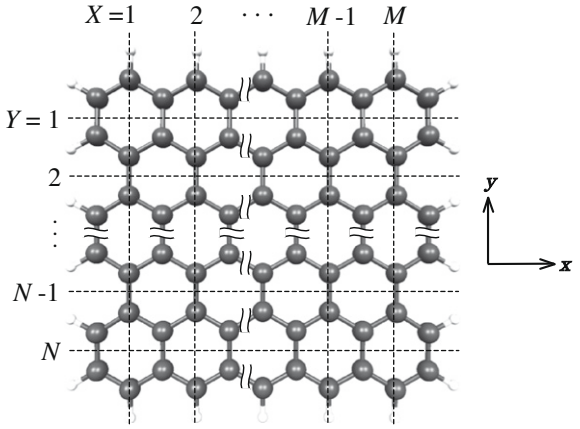

Fig. 1. Definition of rectangular polycyclic aromatic hydrocarbons, PAH[X,Y], where X and Y indicate the lengths (the numbers of fused benzene rings: $X = 1, \ldots, M$ and $Y = 1, \ldots, N$) of zigzag and armchair edges, respectively. Carbon (C) and hydrogen (H) atoms are shown in black and white, respectively.

2.2. Methods for calculating and analyzing γ

Following previous studies [33,38], the UBHandHLYP method [45] was employed because it can semi-quantitatively reproduce the γ values calculated using higher-order electron-correlated methods, e.g., spin-unrestricted coupled cluster singles and doubles with a perturbative triples correction, for diradical molecules with intermediate and large diradical characters. Two diagonal components of γ were calculated, γ_{xxxx} and γ_{yyyy}, where x and y are parallel to the zigzag and armchair edges, respectively.

For the rectangular PAHs, the effect of spin polarization at the zigzag edges on γ can be elucidated by comparing the γ_{yyyy} values of PAH[X,Y] with different Y values for a constant X. Indeed, the diradical character reflects the degree of spatial separation of the α and β distributions into the top- and bottom-zigzag edge regions and γ_{yyyy} is predicted to be affected in contrast to γ_{xxxx}. As shown in Ref. [39], for PAH[3,3] with intermediate diradical character ($y_0 = 0.510$), γ_{yyyy} exceeds γ_{xxxx}, whereas for PAH[5,5] with nearly pure diradical character ($y_0 = 0.989$), both components have similar amplitudes. For larger rectangular PAHs with $y_0 \sim 1$, the γ_{yyyy} is predicted to depend on the next diradical character, y_1, because y_1 indicates the degree of spin polarization related to HOMO-1 and LUMO+1 [see Eqs. (1) and (2)] and could take intermediate values for several larger PAHs.

According to our previous studies, the standard 6-31G* basis set is employed since it is known to be adequate for semi-quantitative comparisons of, at least, the dominant γ components (γ_{iiii}) for rel-

Table 1
Diradical characters (y_0 and y_1)[b] and second hyperpolarizabilities (γ_{xxxx} and γ_{yyyy})[a] [$\times 10^4$ a.u.] for PAH[X,Y] in the singlet states.

System	y_0	y_1	γ_{xxxx}	γ_{yyyy}
PAH[1,1]	0.000	0.000	0.032	0.032
PAH[2,1]	0.050	0.016	0.305	0.090
PAH[3,1]	0.149	0.022	1.52	0.160
PAH[4,1]	0.282	0.034	7.48	0.591
PAH[5,1]	0.419	0.068	19.8	0.730
PAH[6,1]	0.559	0.118	47.3	0.748
PAH[7,1]	0.696	0.183	99.3	0.667
PAH[1,3]	0.037	0.012	0.051	1.73
PAH[2,3]	0.217	0.022	0.409	4.30
PAH[3,3]	0.510	0.053	3.41	14.5
PAH[4,3]	0.806	0.137	15.0	7.33
PAH[5,3]	0.922	0.259	41.2	5.51
PAH[6,3]	0.972	0.407	79.3	7.33
PAH[7,3]	0.995	0.560	123	9.29
PAH[1,5]	0.069	0.014	0.068	11.5
PAH[2,5]	0.372	0.057	0.928	80.3
PAH[3,5]	0.808	0.100	5.36	50.0
PAH[4,5]	0.953	0.233	21.9	25.2
PAH[5,5]	0.989	0.420	49.9	40.5
PAH[6,5]	0.999	0.623	82.5	57.2
PAH[7,5]	0.999	0.790	152	56.0
PAH[1,7]	0.094	0.026	0.086	37.3
PAH[2,7]	0.487	0.114	1.13	316
PAH[3,7]	0.921	0.152	7.08	102
PAH[4,7]	0.999	0.304	27.5	88.8
PAH[5,7]	0.999	0.534	53.1	197
PAH[6,7]	1.000	0.763	100	215
PAH[7,7]	1.000	0.899	220	147

[a] The diradical characters y_0 are calculated from the occupation numbers of UNOs/6-31G*.
[b] The γ values are calculated by the UBHandHLYP/6-31G* method.

atively large-size diradical systems. We applied the finite-field (FF) approach in order to calculate the static γ_{iiii} values. This approach consists in evaluating the fourth-order energy derivative with respect to the applied external electric field [46]. Field amplitudes were chosen such as to attain a numerical accuracy of 1–3% on the γ_{iiii} value. All calculations were performed using the GAUSSIAN 03 program package [45].

In order to elucidate the spatial contributions of electrons to γ_{iiii}, we performed a γ density [$\rho^{(3)}_{iii}(\mathbf{r})$] analysis [47], which utilizes the third derivative of electron density with respect to the applied field:

$$\rho^{(3)}_{iii}(\mathbf{r}) = \left.\frac{\partial^3 \rho}{\partial F_i \partial F_i \partial F_i}\right|_{\mathbf{F}=0}. \quad (3)$$

Using this density, we can obtain γ by

$$\gamma_{iiii} = -\frac{1}{3!}\int r_i \rho^{(3)}_{iii}(\mathbf{r}) d\mathbf{r}, \quad (4)$$

where r_i denotes the i component of the position vector $\mathbf{r}$. The positive (negative) value of $\rho^{(3)}_{iii}(\mathbf{r})$ multiplied by F_i^3 represents the field-induced increase (decrease) in the charge density in proportion to F_i^3. For the simplest example, i.e., a pair of localized γ_{iiii} densities with positive and negative values, the contribution to γ_{iiii} is positive when the direction from positive to negative γ_{iiii} densities coincides with the positive direction of the i axis. The amplitude of the contribution associated with this pair of $\rho^{(3)}_{iii}(\mathbf{r})$ is also proportional to the distance between them.

3. Results and discussion

3.1. Diradical character and spin density distribution

Table 1 lists the diradical characters y_i (i = 0, 1), which are dominant for the present systems, calculated from the occupation numbers of the HOMO−i and LUMO+i of PAH[X,Y]. Firstly, y_0 and y_1 increase with X when keeping Y constant (= 1, 3, 5, 7) and also with Y when keeping X constant (= 1–7). Moreover, for any system, y_0 is larger than y_1 and the increase in y_0 towards 1 precedes that in y_1. This implies that increasing the PAH size develops two successive diradical characters, growing the tetraradical character. Indeed, PAH[7,7] presents two dominant values of diradical characters, y_0 = 1.000 and y_1 = 0.899, which indicates that this system exhibits a nearly pure tetraradical singlet nature. Similar to the previous results [14,23], the size dependences of y_0 and y_1 for PAHs in Table 1 predict that large size PAH[X,Y] (X, $Y \geqslant \sim 7$) and long acenes PAH[X,1] ($X \gg 7$) are regarded as multiradical singlets. Besides these multiradicals, the PAHs can be grouped in three classes according to their y_0 and y_1: (i) compounds with intermediate y_0

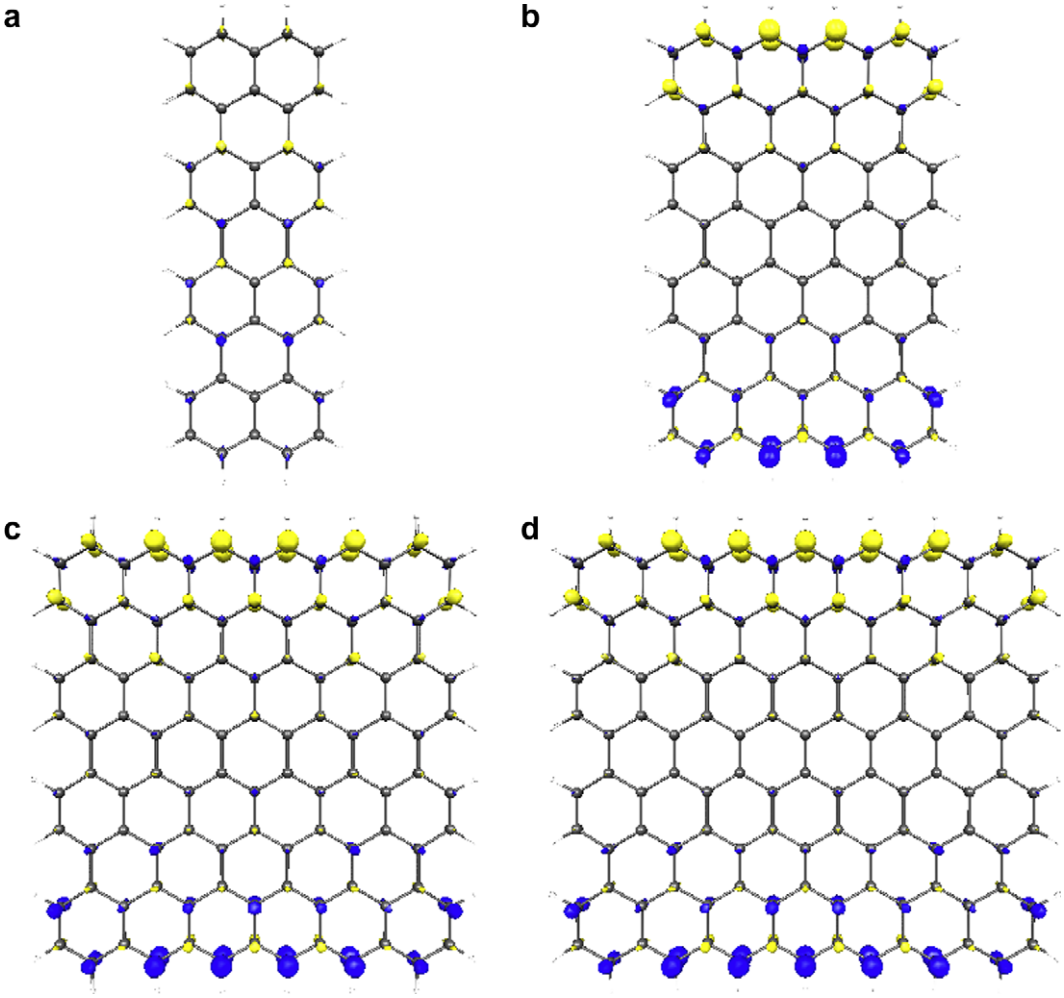

Fig. 2. Spin density distributions of PAH[X,Y] in the singlet state calculated by the UBHandHLYP/6-31G* method: PAH[2,7] (a), PAH[4,7] (b), PAH[6,7] (c) and PAH[7,7] (d). The yellow and blue meshes represent positive and negative densities with iso-surfaces of ±0.025 a.u., respectively. (For interpretation of the references to colour in this figure legend, the reader is referred to the web version of this article.)

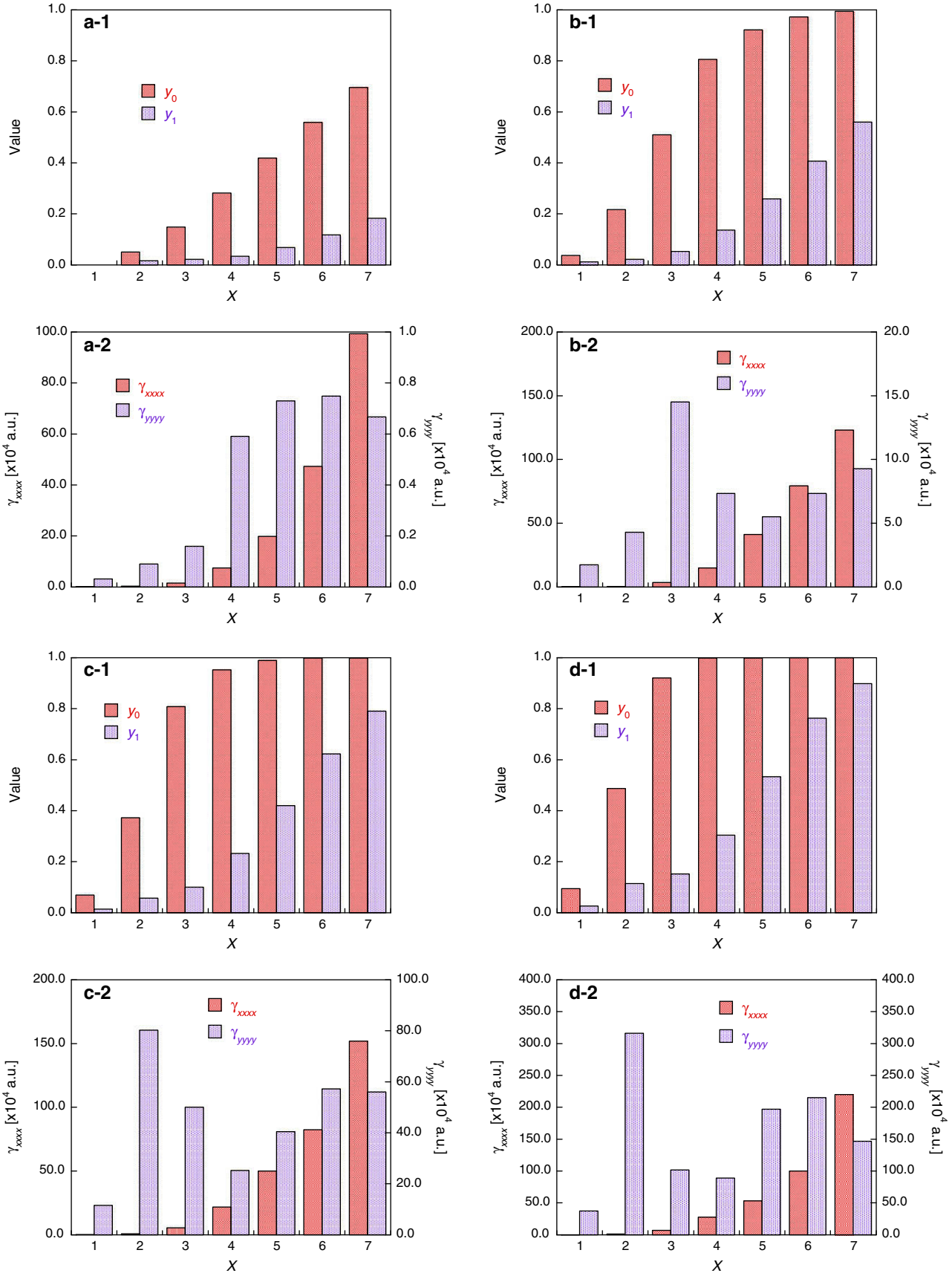

Fig. 3. Diradical characters [y_0 and y_1 (a-1, b-1, c-1, d-1)] and second hyperpolarizabilities [γ_{xxxx} and γ_{yyyy} (a-2, b-2, c-2, d-2)] for PAH[*X*,*Y*] in the singlet states. Here, symbols a, b, c and d represent PAH[*X*,1], PAH[*X*,3], PAH[*X*,5] and PAH[*X*,7], respectively (see Fig. 1).

values {PAH[6,1] (y_0 = 0.559), PAH[3,3] (y_0 = 0.510), PAH[2,5] (y_0 = 0.372) and PAH[2,7] (y_0 = 0.487)}, (ii) those with $y_0 \sim 1$ (pure diradical) and small y_1 values {PAH[5,3] (y_0 = 0.922, y_1 = 0.259), PAH[4,5] (y_0 = 0.953, y_1 = 0.233) and PAH[3,7] (y_0 = 0.921, y_1 = 0.152)}, and (iii) the nanographenes with y_0 close to unity while y_1 presents an intermediate value {PAH[7,3] (y_0 = 0.995, y_1 = 0.560), PAH[6,5] (y_0 = 0.999, y_1 = 0.623) and PAH[6,7] (y_0 = 1.000, y_1 = 0.763)}. These will be related to the variations in γ in the next section.

Fig. 2 shows the spin density distributions of PAH[2,7] (a) (y_0 = 0.487, y_1 = 0.114), PAH[4,7] (b) (y_0 = 0.999, y_1 = 0.304), PAH[6,7] (c) (y_0 = 1.000, y_1 = 0.763) and PAH[7,7] (d) (y_0 = 1.000, y_1 = 0.899) calculated by the UBHandHLYP/6-31G* method. The positive and negative densities, corresponding to α and β spins, in the broken-symmetry spin-unrestricted solutions approximately represent the distribution of unpaired electrons of the system [48]. Except for PAH[2,7], we observe positive and negative spin densities with significant amplitudes on the top- and bottom-zigzag edges as well as those on armchair atoms next to the zigzag edges in contrast to the middle carbon atoms of the armchair edges. This feature is in qualitative agreement with that of PAH[3,3] and PAH[5,5] observed in our previous study [39]. The significant reduction of spin polarization on the zigzag edges as well as the slight emergence of spin polarization in the middle region for PAH[2,7] are attributed to the short zigzag edges, which cannot sustain high diradical character. For PAH[6,7] (c) and PAH[7,7] (d), whose y_1 values are also significant in addition to y_0 = 1, we observe additional spin densities with small amplitudes on the inside zigzag chains (in the fused rings with Y = 1 and 7) next to the zigzag edges as compared to PAH[4,7] having $y_0 \sim 1$ and low y_1 value. These additional spin polarizations are related to the significant y_1 values. Such multiradical character of the PAHs associated with the emergence of odd electron densities on the zigzag edges can also be found to be related to their extra aromatic stabilization originating from the formation of Clar's sextet structures [49], which compensates the destabilization of π-bond cleavages [50].

3.2. Size dependences of γ in relation with the two kinds of diradical characters

Table 1 lists the γ_{xxxx} (along the zigzag edge) and γ_{yyyy} (along the armchair edge) for PAH[X,Y] in their singlet ground state calculated by the UBHandHLYP/6-31G* method. The variations in y_0, y_1, γ_{xxxx} and γ_{yyyy} as a function of X of PAH[X,Y] (Y = 1, 3, 5, 7) are shown in Fig. 3. In agreement with previous result [39], it is found that PAH[6,1] (y_0 = 0.559), PAH[3,3] (y_0 = 0.510), PAH[2,5] (y_0 = 0.372) and PAH[2,7] (y_0 = 0.487), which possess intermediate y_0 values, exhibit the highest γ_{yyyy} responses among the PAH[X, 1], PAH[X, 3], PAH[X, 5] and PAH[X, 7] ($1 \leqslant X \leqslant 7$) families, respectively. In contrast, γ_{xxxx} monotonously increases with X, like in usual π-conjugated systems. The difference in the evolutions of γ_{xxxx} and γ_{yyyy} comes from the difference in spin polarizations between x and y directions [39]. In addition, the PAHs with $Y \geqslant 3$ display another peak in the evolution of γ_{yyyy} with X. These occurs for PAH[6,5] [with $y_0 \sim 1$ and y_1 = 0.623] and for PAH[6,7] [with $y_0 \sim 1$ and y_1 = 0.763] and for PAH[7,3]. The presence of this second peak in γ_{yyyy} as a function of X is now related to y_1 and it corresponds to a region with intermediate y_1 values. Moreover, the γ_{yyyy} peak for the compounds with intermediate y_1 is smaller than that with intermediate y_0 value. This reduced exaltation for y_1 can be associated with the corresponding larger excitation energy, which accounts for smaller γ values as seen from perturbation theory [47]. As a result, the γ_{yyyy} values of increasingly large PAHs ($Y \geqslant 3$) are predicted to exhibit several maxima of which the amplitude decreases with X.

3.3. Signature of the multiradical character in γ density distribution

In order to further address the multiradical character effects on γ, we examine their spatial electronic contributions using the γ density and the natural orbital analyses. Figs. 4 and 5 show the γ_{yyyy} density distributions (calculated by the UBHandHLYP/6-31G* method) and the frontier UNOs (HOMO−1, HOMO, LUMO, LUMO+1) together with the fractional occupation numbers related to the unpaired electrons on both zigzag edges of PAH[3,3] (a) with intermediate y_0 value (y_0 = 0.510, y_1 = 0.053) and PAH[6,7] (b) with intermediate y_1 value (y_0 = 1.000, y_1 = 0.763), respectively. The occupation numbers $n_{\mathrm{HOMO}-i}(n_{\mathrm{LUMO}+i})$ for the occupied(unoccupied) UNOs are smaller(larger) than those of the spin-projected $n_{\mathrm{HOMO}-i}(n_{\mathrm{LUMO}+i})$ [42], given in parentheses, because the spin contamination exaggerates spin polarization at the UHF level of approximation. For both systems, π-electrons provide dominant positive and negative γ_{yyyy} densities, which are well separated to around the bottom- and top-edges, respectively, and both densities rapidly decrease in amplitude toward the middle region. For PAH[3,3], the distribution patterns of γ_{yyyy} densities (Fig. 4a) are shown to be primarily related to the transition density distribution between the HOMO (Fig. 5a-2) and LUMO (Fig. 5a-3). In contrast, for PAH[6,7] the distribution pattern of the γ_{yyyy} density (Fig. 4b) primarily reflects the HOMO−1–LUMO+1 transition density distribution (see Fig. 5b-1 and b-4), while it does not significantly reflect the HOMO–LUMO transition density distribution though the spin polarization distribution obtained from HOMO and LUMO distribu-

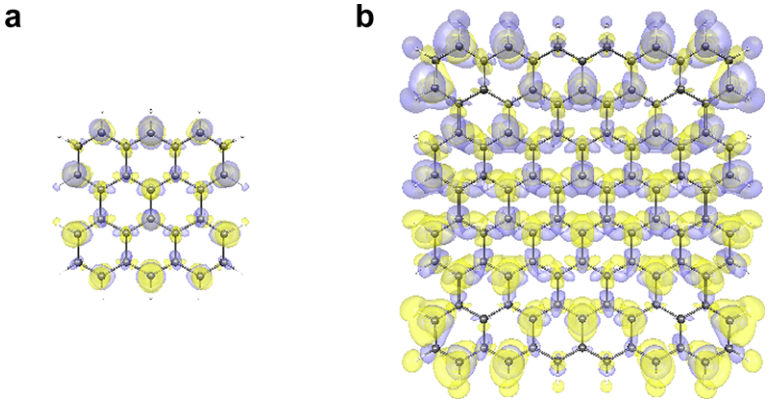

Fig. 4. γ_{yyyy} density distributions of PAH[X,Y] in the singlet state calculated by the UBHandHLYP/6-31G* method: PAH [2,7] (a) and PAH[6,7] (b). The yellow and blue meshes represent positive and negative densities with iso-surface ±500 a.u., respectively. (For interpretation of the references to colour in this figure legend, the reader is referred to the web version of this article.)

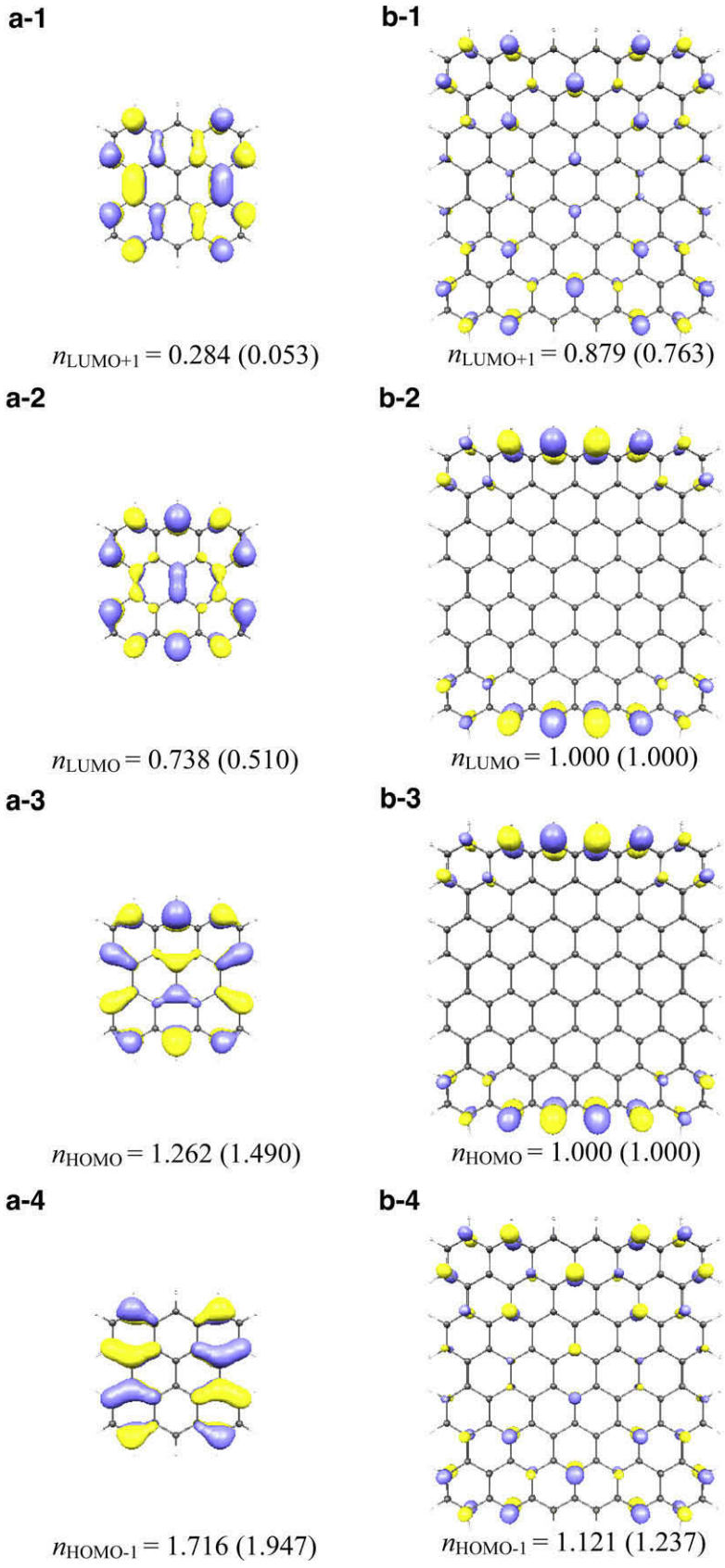

Fig. 5. Frontier UNOs and their occupation numbers (n_{HOMO-i} and n_{LUMO+i}) for PAH[3,3] (a-1, a-2, a-3, a-4) and PAH[6,7] (b-1, b-2, b-3, b-4) calculated by the UHF/6-31G* method. The yellow and blue regions represent positive and negative NOs with contour values of ±0.035 a.u., respectively. The values in parentheses of n_{HOMO-i} and n_{LUMO+i} represent the occupation numbers, i.e., $2 - y_i$ and y_i, respectively, in the spin-projected UHF solutions [42]. (For interpretation of the references to colour in this figure legend, the reader is referred to the web version of this article.)

tions well corresponds to the spin density distribution on zigzag edges (see Figs. 3c and 5b-2 and b-3). These features correspond well to the fact that γ_{yyyy} of PAH[3,3] is determined by the intermediate y_0 value, while that of PAH[6,7] by the intermediate y_1 value since the $y_0 \sim 1$ reduces the HOMO–LUMO contribution. This substantiates the fact that the second γ_{yyyy} peak for PAH[X,Y] ($Y \geqslant 3$) as a function of X originates from the intermediate diradical character y_1. As a result, the first and second γ_{yyyy} peaks, which appear at intermediate y_0 and y_1 values, respectively, for PAH[X,Y] ($Y \geqslant 3$) are an evidence of the multiradical effect (tetraradical in this case) on γ_{yyyy}.

4. Concluding remarks

The present study has investigated the third-order NLO properties of open-shell singlet rectangular graphene nanoflakes (PAHs) by focusing on the multiradical character effect. Indeed, the diradical characters y_0 and y_1 increase with the PAH[X,Y] size so that PAH[X,Y] with X, $Y \geqslant \sim 7$ and acenes PAH[X,1] with $X \gg 7$ can be regarded as multiradical (beyond diradical) singlet systems. As a result, when increasing X and keeping Y fixed, γ_{yyyy} (along the armchair edge) presents maxima that correspond to intermediate y values. The amplitude of these maxima decreases with the order of the diradical character since it is associated with higher energy excitations, e.g., the HOMO−1–LUMO+1 gap (related to y_1) is larger than the HOMO–LUMO gap (related to y_0). In contrast, γ_{xxxx} (along the zigzag edge) shows a monotonous increase with X (keeping Y constant). These results indicate that, in addition to the γ enhancement related to intermediate y_0 values, the multiradical character of graphene nanoflakes is at the origin of additional exaltations of the third-order NLO response. These findings are useful not only for constructing a novel guideline for molecular design of highly efficient NLO materials but also for developing an experimental way to capture the multiradical character signature in graphene nanoflakes.

Acknowledgements

This work was supported by Grant-in-Aid for Scientific Research (Nos. 21350011 and 20655003) and 'Japan-Belgium Cooperative Program' (J091102006) from Japan Society for the Promotion of Science (JSPS), Grant-in-Aid for Scientific Research on Priority Areas (Nos. 18066010, 20038012 and 20350002) from the Ministry of Education, Culture, Sports, Science and Technology (MEXT), and the global COE (center of excellence) program 'Global Education and Research Center for Bio-Environmental Chemistry' of Osaka University. Theoretical calculations were (partly) performed using Research Center for Computational Science, Okazaki, Japan. E.B. thanks the Interuniversity Attraction Pole on 'Functional Supramolecular Systems' (IUAP No. P6-27) for her postdoctoral grant. This work has also been supported by the Academy Louvain (ARC 'Extended π-Conjugated Molecular Tinkertoys for Optoelectronics, and Spintronics').

References

[1] K.S. Novoselov, A.K. Geim, et al., Science 306 (2004) 666.
[2] J.C. Meyer, A.K. Geim, et al., Nature 446 (2007) 60.
[3] K.S. Novoselov, A.K. Geim, et al., Nature 438 (2005) 197.
[4] K.S. Novoselov, Z. Jiang, et al., Science 315 (2007) 1379.
[5] Y.-W. Son, M.L. Cohen, S.G. Louie, Nature 444 (2006) 347.
[6] A.K. Geim, K.S. Novoselov, Nat. Mater. 6 (2007) 183.
[7] K. Kobayashi, Phys. Rev. B 48 (1993) 1757.
[8] D.J. Klein, Chem. Phys. Lett. 217 (1994) 261.
[9] M. Fujita, K. Wakabayashi, K. Nakada, K. Kusakabe, J. Phys. Soc. Jpn. 65 (1996) 1920.
[10] K. Nakada, M. Fujita, G. Dresselhaus, M.S. Dresselhaus, Phys. Rev. B 54 (1996) 17954.
[11] M. Bendikov, H.M. Duong, et al., J. Am. Chem. Soc. 126 (2004) 7416.
[12] Y.W. Son, M.L. Cohen, S.G. Louie, Phys. Rev. Lett. 97 (2006) 216803.
[13] O. Hod, V. Barone, J.E. Peralta, G.E. Scuseria, Nano Lett. 7 (2007) 2295.
[14] J. Hachmann, J.J. Dorando, et al., J. Chem. Phys. 127 (2007) 134309.
[15] L. Pisani, J.A. Chan, B. Montanari, N.M. Harrison, Phys. Rev. B 75 (2007) 064418.
[16] A.H. Castro Neto, F. Guinea, N.M.R. Peres, K.S. Novoselov, A.K. Geim, Rev. Mod. Phys. 81 (2009) 109.
[17] S. Latil, L. Henrard, Phys. Rev. Lett. 97 (2006) 036803.
[18] W.L. Wang, S. Meng, E. Kaxiras, Nano Lett. 8 (2008) 241.
[19] O.V. Yazyev, W.L. Wang, S. Meng, E. Kaxiras, Nano Lett. 8 (2008) 766.
[20] M. Ezawa, Physica E 40 (2008) 1421.
[21] M. Ezawa, Phys. Rev. B 76 (2007) 245415.
[22] J.-F. Rossier, J.J. Palacios, Phys. Rev. Lett. 99 (2007) 177204.
[23] J.R. Dias, Chem. Phys. Lett. 467 (2008) 200.
[24] M. Vandescuren, P. Hermet, V. Meunier, L. Henrard, Ph. Lambin, Phys. Rev. B 78 (2008) 195401.
[25] D.-E. Jiang, S. Dai, J. Phys. Chem. A 112 (2008) 332.
[26] Z. Chen, D.-E. Jiang, et al., Org. Lett. 9 (2007) 5449.
[27] I. Ratera et al., Chem. Phys. Lett. 363 (2002) 245.
[28] M. Nakano, T. Nitta, K. Yamaguchi, B. Champagne, E. Botek, J. Phys. Chem. A 108 (2004) 4105.
[29] Y.Q. Qiu, H.L. Fan, S.L. Sun, C.G. Liu, Z.M. Su, J. Phys. Chem. A 112 (2008) 83.
[30] Z.J. Li et al., PCCP 11 (2009) 402.
[31] P.C. Jha, Z. Rinkevicius, H. Ågren, ChemPhysChem 10 (2009) 817.
[32] D.A. Dougherty, Acc. Chem. Res. 24 (1991) 88.
[33] M. Nakano, R. Kishi, et al., J. Phys. Chem. A 109 (2005) 885.
[34] M. Nakano, R. Kishi, et al., J. Chem. Phys. 125 (2006) 074113.
[35] M. Nakano, R. Kishi, et al., Phys. Rev. Lett. 99 (2007) 033001.
[36] M. Nakano, K. Yoneda, et al., J. Chem. Phys. 131 (2009) 114316.
[37] M. Nakano, T. Kubo, et al., Chem. Phys. Lett. 418 (2006) 142.
[38] M. Nakano, R. Kishi, et al., J. Phys. Chem. A 110 (2006) 4238.
[39] M. Nakano, H. Nagai, et al., Chem. Phys. Lett. 467 (2008) 120.
[40] K. Yoneda, M. Nakano, et al., Chem. Phys. Lett. 480 (2009) 278.
[41] K. Kamada, K. Ohta, et al., Angew. Chem., Int. Ed. 46 (2007) 3544.
[42] K. Yamaguchi, in: R. Carbo, M. Klobukowski (Eds.), Self-Consistent Field: Theory and Applications, Elsevier, Amsterdam, 1990, p. 727.
[43] S. Yamanaka, M. Okumura, M. Nakano, K. Yamaguchi, J. Mol. Struct. 310 (1994) 205.
[44] D. Herebian, K.E. Wieghardt, F. Neese, J. Am. Chem. Soc. 125 (2003) 10997.
[45] M. J. Frisch et al., Gaussian 03, Revision C.02, Gaussian Inc., Pittsburgh, PA, 2004.
[46] H.D. Cohen, C.C.J. Roothaan, J. Chem. Phys. 43 (1965) S34.
[47] M. Nakano, I. Shigemoto, S. Yamada, K. Yamaguchi, J. Chem. Phys. 103 (1995) 4175.
[48] K. Takatsuka, T. Fueno, K. Yamaguchi, Theoret. Chim. Acta 48 (1978) 175.
[49] E. Clar, The Aromatic Sextet, John Wiley and Sons, London, 1972.
[50] A. Shimizu, Y. Hirao, T. Kubo et al., in: G. Maroulis, T. Simos (Eds.), Computational Methods in Science and Engineering, Theory and Computation, AIP Conference Proceedings, in press.